



# HHS Public Access

Author manuscript

*Dev Dyn.* Author manuscript; available in PMC 2020 September 01.

Published in final edited form as:

*Dev Dyn.* 2019 September ; 248(9): 762–770. doi:10.1002/dvdy.66.

## Functional analysis of Aarf domain-containing kinase 1 in *Drosophila melanogaster*

Dona R. Wisidagama, Stefan M. Thomas, Geanette Lam, Carl S. Thummel

Department of Human Genetics, University of Utah School of Medicine, Salt Lake City, Utah

### Abstract

**Background:** The ADCK proteins are predicted mitochondrial kinases. Most studies of these proteins have focused on the Abc1/Coq8 subfamily, which contributes to Coenzyme Q biosynthesis. In contrast, little is known about ADCK1 despite its evolutionary conservation in yeast, *Drosophila*, *Caenorhabditis elegans* and mammals.

**Results:** We show that *Drosophila ADCK1* mutants die as second instar larvae with double mouth hooks and tracheal breaks. Tissue-specific genetic rescue and RNAi studies show that *ADCK1* is necessary and sufficient in the trachea for larval viability. In addition, tracheal-rescued *ADCK1* mutant adults have reduced lifespan, are developmentally delayed, have reduced body size, and normal levels of basic metabolites.

**Conclusion:** The larval lethality and double mouth hooks seen in *ADCK1* mutants are often associated with reduced levels of the steroid hormone ecdysone, suggesting that this gene could contribute to controlling ecdysone levels or bioavailability. Similarly, the tracheal defects in these animals could arise from defects in intracellular lipid trafficking. These studies of *ADCK1* provide a new context to define the physiological functions of this poorly understood member of the ADCK family of predicted mitochondrial proteins.

### Keywords

metabolism; mitochondria; molting; trachea

## INTRODUCTION

Mitochondria are an important organelle in all eukaryotic cells. Not only are they the main source for cellular energy production, but they are also important for critical cellular functions such as calcium homeostasis, lipid homeostasis, and metabolite synthesis.<sup>1,2</sup> Consistent with this, mitochondrial dysfunction is associated with aging and a plethora of metabolic disorders including cancer, neurodegeneration, diabetes, and inborn errors of metabolism.<sup>3,4</sup> These important roles for mitochondria have led to extensive research using multiple model systems, providing insights into mitochondrial activities and their impact on cellular and organismal growth, development, and physiology.<sup>5</sup> In spite of these efforts, however, about a fifth of the mitochondrial proteome remains largely uncharacterized.<sup>1,5</sup>

---

**Correspondence:** Carl S. Thummel, Department of Human Genetics, University of Utah School of Medicine, Salt Lake City, UT 84112-5330. cthummel@genetics.utah.edu.

This includes many proteins that are highly conserved throughout eukaryotic organisms, a strong indication that they perform fundamentally important functions.

In this study, we examine the ADCK family of predicted mitochondrial kinases, represented by ADCK1–5 in humans (Figure 1). Most studies have centered on the ABC1/Coq8 subfamily, which includes ABC1/Coq8 in yeast and human ADCK3 and ADCK4.<sup>6</sup> Coq8 is part of a multiprotein complex involved in the biosynthesis of Coenzyme Q (CoQ), which is a lipid that resides in the mitochondrial inner membrane and contributes to electron transport. Loss of *ADCK3* in humans is associated with an inherited form of ataxia accompanied by CoQ deficiency.<sup>7–10</sup> A recent biochemical study has shown that ADCK3 can bind ATP and adopt an atypical protein kinase-like fold that is blocked by autoinhibitory domains, providing initial insights into its molecular function.<sup>11</sup> Mutations in *ADCK4* are associated with steroid-resistant nephrotic syndrome in humans as well as reduced levels of CoQ.<sup>12,13</sup> In spite of multiple studies, however, the molecular functions of Coq8 and its human counterparts remain unclear.<sup>14</sup> In addition, ADCK2 and ADCK5 are largely uncharacterized.

One study has reported a role for *ADCK1* in yeast. These investigators found that overexpression of yeast *ADCK1* (referred to as *Mcp2* in this study) can rescue the growth defects of mutants in *Mdm10*, which encodes part of the ERMES complex.<sup>15</sup> This multiprotein complex tethers the endoplasmic reticulum to mitochondria and is required to maintain mitochondrial lipid homeostasis.<sup>16</sup> ADCK1 localizes to the inner membrane of mitochondria and does not directly associate with the ERMES complex. *ADCK1* overexpression, however, can restore the membrane lipid defects in *mdm10* mutants as well as rescue this phenotype in mutants for other ERMES complex members. The authors propose that ADCK1 has a redundant role with the ERMES complex in maintaining proper mitochondrial lipid levels.<sup>15</sup> ERMES complex components, however, have not been found in metazoans to date.<sup>16</sup> In addition, the molecular roles of ADCK1 remain uncharacterized. Here we present a genetic analysis of *ADCK1* in *Drosophila* in an effort to define its roles during development.

We show that *Drosophila ADCK1* mutants display larval lethality and double mouth hooks, which are hallmarks of molting defects and often associated with reduced levels of the steroid hormone ecdysone.<sup>17</sup> Mutants for *ADCK1* also display tracheal breaks and the re-expression of *ADCK1* in tracheal tissue is sufficient to rescue their larval lethality, demonstrating an essential role for the gene in this tissue. The rescued adults, however, have a reduced lifespan, delayed development, and reduced body size, indicating that *ADCK1* also has functions outside the trachea. These studies provide a foundation for understanding the roles of *ADCK1* during larval and adult *Drosophila* development.

## 2 | RESULTS

### 2.1 | ADCK1 is conserved through evolution

To investigate the evolutionary conservation of ADCK family members we generated a phylogenetic tree using maximum likelihood analysis (Figure 1). The ADCK family of predicted kinases includes Ylr253, Ypl109, and ABC1/Coq8 (Ygl119) in yeast, CG3608,

CG32649, and CG7616 in *Drosophila*, ADCK1–5 in mammals, and D2023.6, Y32H12A.7, and C35D10.4 in *Caenorhabditis elegans*. ABC1/Coq8 is most similar to CG32649 in *Drosophila*, C35D10.4 in *C. elegans*, and ADCK3 and ADCK4 in mammals. Yp1109 is most similar ADCK2 and Y32H12A.7 in *C. elegans*. ADCK5 is a homolog of CG7616 in *Drosophila* and more distantly related to Ylr253 in yeast. Our studies are focused on ADCK1, designated CG3608 in *Drosophila*. Although this protein is highly conserved through evolution (48% amino acid identity between fly and human), its function remains poorly understood. As a first step toward defining the functional role of *ADCK1* in *Drosophila*, we generated deletions in this locus using CRISPR-Cas9.

## 2.2 | *Drosophila ADCK1* mutants are larval lethal

Two deletion mutations were generated in the *ADCK1* locus, designated *ADCK1*<sup>1</sup> and *ADCK1*<sup>2</sup>. *ADCK1*<sup>1</sup> consists of an ~1.5 kb deletion that removes part of the 5' UTR, the start codon, and most of the protein coding sequence (Figure 2A). *ADCK1*<sup>2</sup> is an overlapping deficiency that removes the coding region for the N-terminal portion of the protein (Figure 2A). Transheterozygous mutants carrying both alleles die as second instar larvae, with approximately 85% (n = 34) of the animals displaying double mouth hooks, indicative of a molting defect (Figure 2B,C). The remaining animals complete the molt and display only the second instar larval mouth hooks. Similar lethal phenotypes are seen when *ADCK1*<sup>1</sup> homozygous mutants are analyzed. Additionally, mutant larvae appear to suffer from hypoxic stress and prematurely wander away from the food.<sup>18</sup> Consistent with this, *ADCK1* mutants display breaks in the dorsal tracheal trunks (Figure 2D,E). Both larval molting defects and tracheal breaks are associated with changes in ecdysone signaling, suggesting that ADCK1 may play a role in cholesterol homeostasis, sterol trafficking, or steroid hormone production.<sup>17,19,20</sup> Feeding 20-hydroxyecdysone to *ADCK1* mutant larvae, however, had no effects on molting or viability, suggesting that ecdysone titers are not limiting.

## 2.3 | *ADCK1* is required in trachea for larval growth and development

To investigate the tissue-specific functions of *ADCK1*, we expressed the wild-type gene in *ADCK1* mutants using the GAL4/UAS system.<sup>21</sup> Expression of *ADCK1* in the fat body (*cg-GAL4*, *r4-GAL4*), intestine (*mex-GAL4*, *npc1b-GAL4*), neurons (*elav-GAL4*) or prothoracic gland (*phm-GAL4*) had no effect on larval viability (Figure 3A). However, expressing *ADCK1* ubiquitously using the *da-GAL4* driver or in the tracheal system using *btl-GAL4* rescued lethality through to adulthood (Figure 3A). Interestingly, the extent of rescue with these two drivers is different, with more complete rescue from the ubiquitous driver than is seen with tracheal-specific expression (Figure 3A). This suggests that, while *ADCK1* expression is sufficient in the trachea for larval development, its activity is required in other tissues for complete viability. Consistent with this, *ADCK1* is expressed widely in *Drosophila*, with higher levels in the adult intestine, fat body, and heart.<sup>22</sup>

To investigate whether ADCK1 is necessary in trachea for larval viability we performed tissue-specific RNAi studies. Consistent with our genetic rescue results, ubiquitous loss of *ADCK1* using the *da-GAL4* driver resulted in fully penetrant lethality (100%, n = 725). Lethality was also seen with *btl-GAL4* driving *ADCK1* RNAi (100%, n = 382), as well as

with a different *ADCK1* RNAi line (VDRC; 100%, n = 282). The *btl* > *ADCK1-RNAi* animals arrested their development as either first instar larvae (67%) or second instar larvae (33%, n = 30). They did not, however, display double mouth hooks, suggesting that this mutant phenotype arises from a loss of *ADCK1* activity outside the trachea. Additionally, *btl* > *ADCK1-RNAi* larvae display tracheal abnormalities, which includes tracheal breaks and lumen separation (Figure 3B–D). Consistent with these morphological defects, these larvae prematurely wander away from the food possibly due to hypoxic stress. Taken together, our tissue-specific genetic rescue and RNAi studies suggest that *ADCK1* is necessary and sufficient in the trachea for larval viability and growth as well as tracheal integrity.

#### 2.4 | Tracheal-rescued *ADCK1* mutants are small and have a reduced lifespan

Phenotypic characterization of *ADCK1* mutants is complicated by their lethality as early second instar larvae. We thus took advantage of the mutants rescued to adulthood to conduct initial functional studies of *ADCK1* outside of trachea. In particular, we were interested in examining the possibility that *ADCK1* might contribute to longevity and systemic metabolism given its mitochondrial localization and expression in the fat body and intestine, which play central roles in maintaining metabolic homeostasis.

As a first step toward this goal, we examined the lifespan of tracheal-rescued *ADCK1* mutants. Both male and female rescued *ADCK1* mutants display a reduced lifespan relative to controls (Figure 4A,B). Interestingly, the ubiquitous rescue of *ADCK1* is more efficient at extending lifespan than tracheal-specific rescue. This supports our tissue-specific genetic rescue studies and suggests that *ADCK1* has important activities outside of the trachea that are required for the overall health of the animal. In addition, we noticed that tracheal-rescued animals eclose approximately 2 days later than controls and this developmental delay can be rescued by ubiquitous *ADCK1* expression using *da-GAL4* (Figure 5A). Delayed development is often accompanied by a reduction in body size and, consistent with this, pupal body size is reduced in tracheal-rescued mutants (Figure 5B). In addition, tracheal-rescued *ADCK1* mutant adults have reduced protein levels in both males and females (Figure 5C,D), further supporting a role for *ADCK1* in growth during larval stages.

To address possible metabolic functions for *ADCK1*, we assayed the major forms of stored energy in tracheal-rescued mutants, stored carbohydrates in the form of glycogen and stored lipids as triglycerides, as well as free glucose (Figure 6A–D). None of these metabolites, however, are affected in tracheal-rescued *ADCK1* mutants, suggesting that this gene does not play a critical role in maintaining adult metabolic homeostasis under normal feeding conditions.

### 3 | DISCUSSION

In this study, we present a functional analysis of *ADCK1* during development. *Drosophila ADCK1* mutants die as second instar larvae with molting defects and tracheal breaks, each of which is associated with reduced signaling by the steroid hormone ecdysone.<sup>17,19,20</sup> *ADCK1* does not, however, appear to impact systemic sterol levels since we cannot rescue the mutants with dietary ecdysone, which is a standard test for phenotypes caused by a reduced ecdysone titer. In addition, specific expression of wild-type *ADCK1* in the

prothoracic glands of *ADCK1* mutants, where ecdysone is produced, has no effect on larval viability, suggesting that this gene has no role in ecdysteroid biosynthesis. Rather, considering that *ADCK1* could encode a lipid kinase like other ADCK family members, one possibility to consider is a role for ADCK1 in phosphorylating ecdysteroids. Ecdysteroid phosphates provide a major source of inactive stored hormone in the yolk granules of insect oocytes.<sup>23–25</sup> Thus, reduced ecdysteroid phosphorylation could lead to increased rather than decreased titers of active hormone in *ADCK1* mutants. Consistent with this model, increased ecdysone signaling leads to a shortened lifespan in *Drosophila*, similar to the effects we see on lifespan in rescued *ADCK1* mutants.<sup>26,27</sup> An alternative model to consider is that *ADCK1* mutants suffer from defects in intracellular sterol trafficking. Mutants for the *Drosophila* Niemann-Pick Disease gene *npc1a*, which is required for intracellular cholesterol trafficking, die as first instar larvae with reduced ecdysteroid titers.<sup>28,29</sup> Direct ecdysone titer measurements in *ADCK1* mutants would provide a means of testing these models and gaining further insights into *ADCK1* function in *Drosophila*.

Our tissue-specific genetic rescue and RNAi studies indicate the *ADCK1* is both necessary and sufficient in the trachea for viability. It remains unclear, however, how the tracheal expression of wild-type *ADCK1* can rescue the molting defects and second instar lethality since these are not known to be associated with tracheal function. It is also worth noting that ubiquitous expression of wild-type *ADCK1* in mutants is more efficient at rescuing larval viability and lifespan than tracheal-specific expression, suggesting that *ADCK1* has important functions in peripheral tissues. Further studies could address this in more detail, including systematic *ADCK1* RNAi studies using a range of tissue-specific GAL4 drivers. More detailed phenotypic characterization of the tracheal-rescued *ADCK1* mutants could address if the partial lethality and/or developmental delay seen in these animals is due to a reduced ecdysone titer arising from *ADCK1* activity outside the trachea. One interesting model to consider in this regard is a potential role for Shade, which is a mitochondrial enzyme that catalyzes the conversion of ecdysone to active 20-hydroxyecdysone (20E) in peripheral tissues.<sup>30</sup> Roles for ADCK1 in 20E production could be addressed by determining the levels of sterol intermediates in tracheal-rescued *ADCK1* mutants, including ecdysone and 20E.

The requirement for *ADCK1* in tracheal molting and morphology are consistent with the known roles for lipid metabolism in tracheal development. The fatty acyl-CoA reductase encoded by the *waterproof* locus is required for gas filling of the trachea at the molts, and lipoprotein-mediated lipid uptake is necessary for the proper structure of the tracheal lumen.<sup>31,32</sup> In addition, lipid phosphate phosphatases encoded by the *Drosophila* Wunen family are required for normal tracheal development during embryogenesis.<sup>33</sup> These enzymes are integral membrane proteins that catalyze the dephosphorylation of a wide range of lipid phosphates.<sup>34</sup> Given that functional studies of *ADCK1* in yeast have implied a role for this putative lipid kinase in intracellular lipid trafficking, it is interesting to consider that the tracheal defects in *Drosophila ADCK1* mutants could arise from a defect in this process.<sup>15</sup> Further studies are required to determine if *ADCK1* contributes to lipid uptake or intracellular lipid trafficking in the trachea, and if these activities could explain the tracheal defects that we observe in *ADCK1* mutant larvae. Finally, it should be noted that, as this study was in its final stages of revision, an article was published describing roles for

*Drosophila ADCK1* in the muscle.<sup>35</sup> This study supports and extends the work shown here by demonstrating roles for this gene in mitochondrial function and motility.

Taken together, our work in *Drosophila* establishes a requirement for *ADCK1* in tracheal development and larval molting, both of which are consistent with a role for this predicted mitochondrial kinase in sterol modifications and/or intracellular lipid trafficking. In addition, our characterization of tracheal-rescued *ADCK1* mutant adults has revealed roles for this gene in lifespan, developmental timing, and overall growth. These studies provide a new context to define the molecular functions of *ADCK1* as well as directions for future work that could enhance our understanding of this poorly studied member of the ADCK family of mitochondrial proteins.

## 4 | EXPERIMENTAL PROCEDURES

### 4.1 | *Drosophila* strains and media

*Drosophila* was raised at 25 °C on media containing 8% yeast, 9% sugar, and 1% agar. Larval experiments were performed on egg caps containing grape juice supplemented with yeast paste. All genetic studies were performed using a transheterozygous combination of *w<sup>1118</sup>*; *ADCK1<sup>1</sup>* and *w<sup>1118</sup>*; *ADCK2* alleles. *w<sup>1118</sup>*; *ADCK1<sup>1</sup>/+* transheterozygotes were used as a control genotype.

### 4.2 | Generation of *ADCK1* deletion mutants

Mutations in *Drosophila ADCK1* were generated using CRISPR-Cas9 as described.<sup>36</sup> Our strategy resulted in two overlapping deletions in the *ADCK1* locus, with the deleted region replaced by an eye-specific *DsRed* reporter to facilitate the identification of targeted mutants (Figure 2A). The *3XP3-DsRed* marker was inserted in an opposite orientation from *ADCK1*. *ADCK1<sup>1</sup>* consists of a 1553 bp deletion and *ADCK1<sup>2</sup>* carries a 323 bp deletion. Guide RNAs for *ADCK1<sup>1</sup>*: 5' guide GTGAAAGCCCAAAGGTTAATCGG, 3' guide GAACCGGATGACCGCCTTCTGGG. Guide RNAs for *ADCK1<sup>2</sup>*: 5' guide GCCAAAATCAGTCAGCGGAGGG, 3' guide GGAACTTTACTACAGGGAATGG. Both *ADCK1<sup>1</sup>* and *ADCK1<sup>2</sup>* mutants were outcrossed to *w<sup>1118</sup>* to provide a consistent genetic background for functional studies.

### 4.3 | Generation of the *UAS-ADCK1* transgenic flies

The *ADCK1* coding region was amplified from the plasmid (DGRC SD09850) using the forward primer AAGCGAATT CATGCTGTTGCGTCGCGTTCTGGGC and reverse primer AAGCGGTACCCTAAATAACCTGCTTGAGAGCTTCAA G. The *ADCK1* cDNA amplicon was digested with EcoR1 and Kpn1 and then inserted into the pUAST-attB plasmid digested with the same enzymes. The presence of the *ADCK1* cDNA in the pUAST-attB plasmid was verified by restriction digestion and DNA sequencing. The final *UAS-ADCK1* transgene was inserted into the fly genome at the attP40 site on the second chromosome.<sup>37</sup>



#### 4.4 | Phylogenetic reconstruction

NCBI genome sequence databases were queried to obtain the peptide sequences for human ADCK proteins as well as the homologous yeast, *C. elegans* and *D. melanogaster* ADCK protein sequences. Protein FASTA sequences were aligned using MUSCLE (Multiple Sequence Comparison by Log Expectation) and the aligned peptide sequences were uploaded to MEGA7 to obtain a maximum likelihood phylogram.<sup>38</sup>

#### 4.5 | Tissue-specific genetic rescue studies

The deletion line  $w^{1118}; ADCK1^2$  was recombined with the *UAS-ADCK1* rescue construct, which is also on the second chromosome, and maintained with a *CyO* balancer. This stock was crossed to  $w^{1118}; ADCK1^1 / CyO$  animals carrying different tissue-specific GAL4 drivers in the same genetic background. To calculate the efficiency of rescue with each GAL4 driver, we compared the proportion of surviving rescued animals to the expected Mendelian ratio, assuming a complete rescue. Since the *ADCK1* mutant males and females used for each cross carry a *CyO* balancer, the expected Mendelian ratio for complete rescue in their offspring would be 33% of the final population lacking *CyO* (rescued *ADCK1*<sup>1</sup>/*ADCK1*<sup>2</sup> mutants), with the remaining 66% of the population carrying the *CyO* balancer (*ADCK1*<sup>1</sup>/*CyO* or *ADCK1*<sup>2</sup>/*CyO*). Eggs were collected on grape juice caps overnight and 200 eggs were transferred to standard food vials. Surviving adults were scored for the presence or absence of the *CyO* balancer.

#### 4.6 | Developmental delay

To calculate the developmental delay, each cross was allowed to lay eggs for an 8-hour window. The number of adults that eclosed in that vial was recorded daily. This data was used to calculate the number of days it took for 50% of the population to eclose, as presented in Figure 5A.

#### 4.7 | Pupal size determination

To quantify pupal size, control or tracheal-rescued *ADCK1*<sup>1</sup>/*ADCK1*<sup>2</sup> mutant pupae were removed and placed on a cover slip with double-sided tape. Sixty pupae for each genotype were imaged and the area of each animal was calculated using ImageJ software. The sizes of tracheal-rescued *ADCK1* mutants were normalized to the controls for the figure.

#### 4.8 | Metabolite assays

Adult flies were collected 4 days after eclosion, aged for 7 days, and samples of five flies per replicate were flash frozen in liquid nitrogen. Homogenates prepared from these animals were subjected to metabolite assays as described.<sup>39</sup> Triglyceride measurements were performed using a coupled colorimetric assay (Sigma T2449). Glycogen and glucose concentrations were determined using the hexokinase (HK) and/or glucose oxidase (GO) assay kits (Sigma GAHK20, GAGO20). Total protein levels were determined in parallel by Bradford assay.

## 4.9 | Longevity

For adult lifespan studies, 4-day-old flies were sorted and mated with the opposite sex for 7 days, after which 10–15 flies were transferred to vials containing 8% yeast, 9% sugar. Animals were scored for lethality daily and transferred to fresh food every 2 days.

## 4.10 | Statistics

GraphPad PRISM 6 software was used to plot data and perform statistical analysis. Pairwise comparison *P*-values were calculated using a two-tailed Student's *t*-test unless otherwise specified. Longevity is presented as a Kaplan Meier curve and the *P*-values were determined using a log-rank Mantel-Cox test. Error bars represent the SE of the mean.

## ACKNOWLEDGMENTS

We thank M. Metzstein for helpful discussions and providing the *btl-GAL4, UAS-GFP* stock, A-F. Ruaud and J. McCormick for help with the phylogenetic analysis of ADCK family members, the Bloomington Stock Center for fly stocks (NIH P40OD018537), the Transgenic RNAi Project (TRiP), and FlyBase for informatic support. This work was supported by the NIH (R01GM094232, R01CA228346).

Funding information

National Cancer Institute, Grant/Award Number: R01CA228346; National Institute of General Medical Sciences, Grant/Award Number: R01GM094232

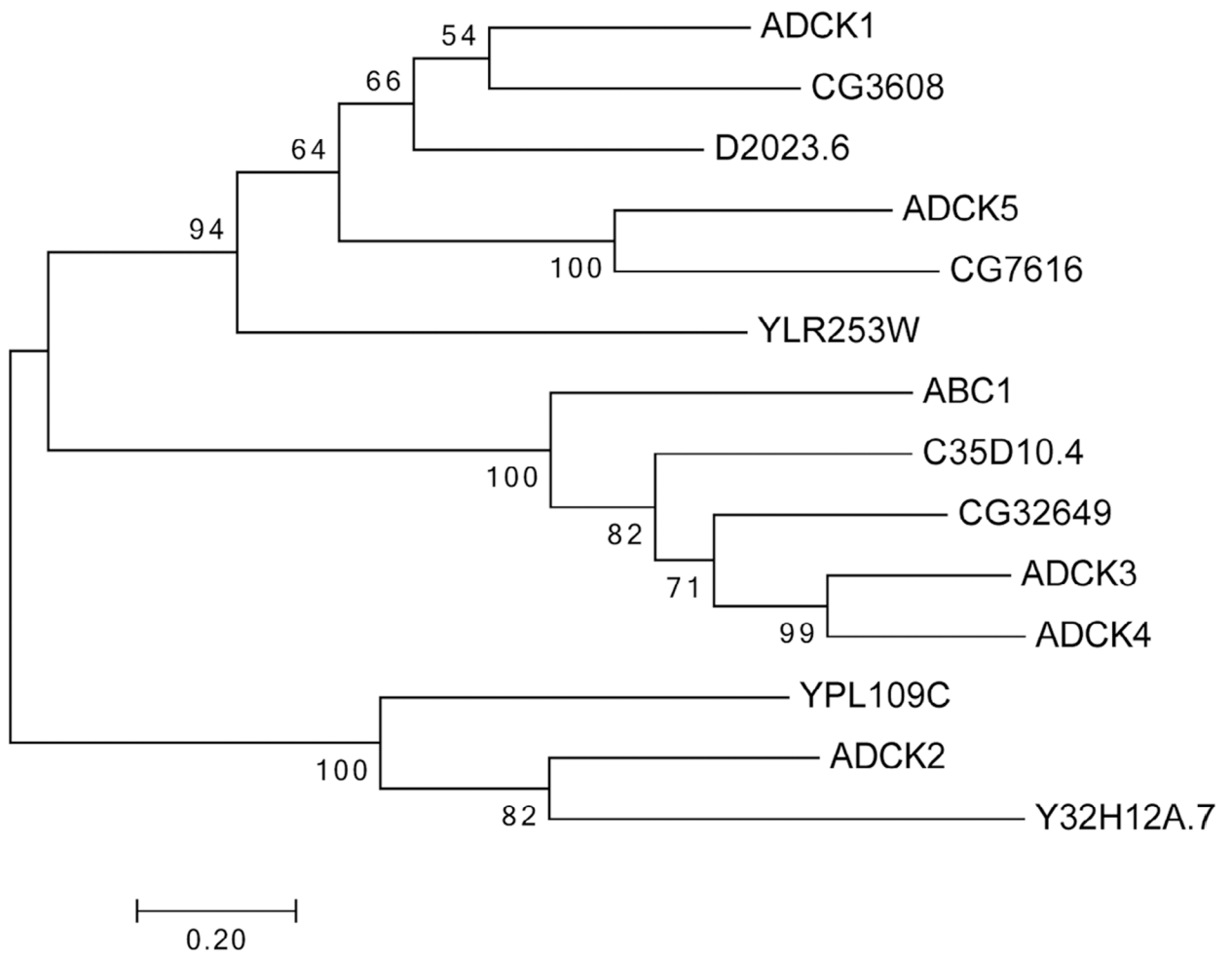
## REFERENCES

- Rutter J, Hughes AL. Power(2): the power of yeast genetics applied to the powerhouse of the cell. *Trends Endocrinol Metab.* 2015;26:59–68. [PubMed: 25591985]
- Spinelli JB, Haigis MC. The multifaceted contributions of mitochondria to cellular metabolism. *Nat Cell Biol.* 2018;20:745–754. [PubMed: 29950572]
- Gray LR, Tompkins SC, Taylor EB. Regulation of pyruvate metabolism and human disease. *Cell Mol Life Sci.* 2014;71:2577–2604. [PubMed: 24363178]
- Wallace DC. A mitochondrial paradigm of metabolic and degenerative diseases, aging, and cancer: a dawn for evolutionary medicine. *Annu Rev Genet.* 2005;39:359–407. [PubMed: 16285865]
- Pagliarini DJ, Rutter J. Hallmarks of a new era in mitochondrial biochemistry. *Genes Dev.* 2013;27:2615–2627. [PubMed: 24352419]
- Acosta MJ, Vazquez Fonseca L, Desbats MA, et al. Coenzyme Q biosynthesis in health and disease. *Biochim Biophys Acta.* 2016; 1857:1079–1085. [PubMed: 27060254]
- Barca E, Musumeci O, Montagnese F, et al. Cerebellar ataxia and severe muscle CoQ10 deficiency in a patient with a novel mutation in ADCK3. *Clin Genet.* 2016;90:156–160. [PubMed: 26818466]
- Cullen JK, Abdul Murad N, Yeo A, et al. AarF domain containing kinase 3 (ADCK3) mutant cells display signs of oxidative stress, defects in mitochondrial homeostasis and lysosomal accumulation. *PLoS One.* 2016;11:e0148213. [PubMed: 26866375]
- Lagier-Tourenne C, Tazir M, Lopez LC, et al. ADCK3, an ancestral kinase, is mutated in a form of recessive ataxia associated with coenzyme Q10 deficiency. *Am J Hum Genet.* 2008;82:661–672. [PubMed: 18319074]
- Mollet J, Delahodde A, Serre V, et al. CABP1 gene mutations cause ubiquinone deficiency with cerebellar ataxia and seizures. *Am J Hum Genet.* 2008;82:623–630. [PubMed: 18319072]
- Stefely JA, Reidenbach AG, Ulbrich A, et al. Mitochondrial ADCK3 employs an atypical protein kinase-like fold to enable coenzyme Q biosynthesis. *Mol Cell.* 2015;57:83–94. [PubMed: 25498144]

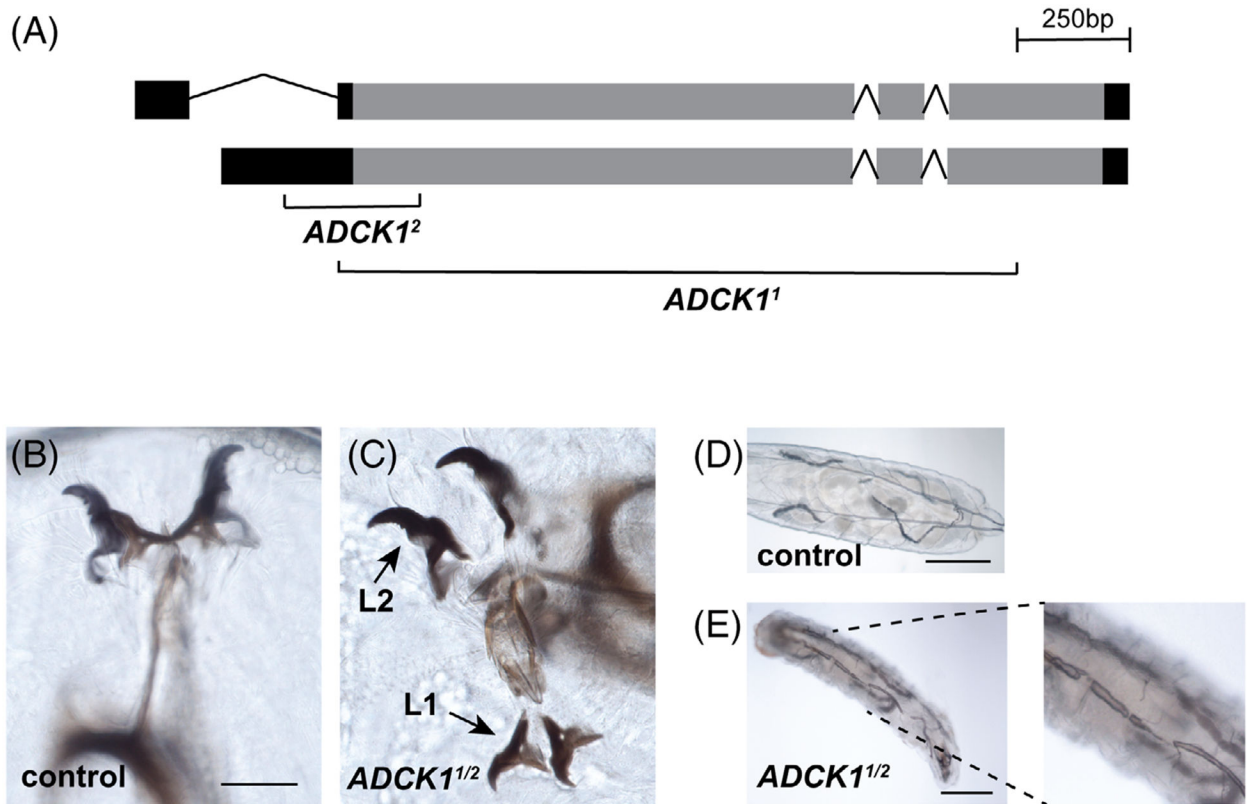


12. Ashraf S, Gee HY, Woerner S, et al. ADCK4 mutations promote steroid-resistant nephrotic syndrome through CoQ10 biosynthesis disruption. *J Clin Invest.* 2013;123:5179–5189. [PubMed: 24270420]
13. Vazquez Fonseca L, Doimo M, Calderan C, et al. Mutations in COQ8B (ADCK4) found in patients with steroid-resistant nephrotic syndrome alter COQ8B function. *Hum Mutat.* 2018;39: 406–414. [PubMed: 29194833]
14. Stefely JA, Licitra F, Laredj L, et al. Cerebellar ataxia and coenzyme Q deficiency through loss of unorthodox kinase activity. *Mol Cell.* 2016;63:608–620. [PubMed: 27499294]
15. Tan T, Ozbalci C, Brugger B, Rapaport D, Dimmer KS. Mcp1 and Mcp2, two novel proteins involved in mitochondrial lipid homeostasis. *J Cell Sci.* 2013;126:3563–3574. [PubMed: 23781023]
16. Kornmann B, Walter P. ERMES-mediated ER-mitochondria contacts: molecular hubs for the regulation of mitochondrial biology. *J Cell Sci.* 2010;123:1389–1393. [PubMed: 20410371]
17. Neubueser D, Warren JT, Gilbert LI, Cohen SM. Molting defective is required for ecdysone biosynthesis. *Dev Biol.* 2005;280: 362–372. [PubMed: 15882578]
18. Wingrove JA, O'Farrell PH. Nitric oxide contributes to behavioral, cellular, and developmental responses to low oxygen in *Drosophila*. *Cell.* 1999;98:105–114. [PubMed: 10412985]
19. Fisk GJ, Thummel CS. The DHR78 nuclear receptor is required for ecdysteroid signaling during the onset of *Drosophila* metamorphosis. *Cell.* 1998;93:543–555. [PubMed: 9604930]
20. Lam G, Hall BL, Bender M, Thummel CS. DHR3 is required for the prepupal-pupal transition and differentiation of adult structures during *Drosophila* metamorphosis. *Dev Biol.* 1999; 212:204–216. [PubMed: 10419696]
21. Caygill EE, Brand AH. The GAL4 system: a versatile system for the manipulation and analysis of gene expression. *Methods Mol Biol.* 2016;1478:33–52. [PubMed: 27730574]
22. Robinson SW, Herzyk P, Dow JA, Leader DP. FlyAtlas: database of gene expression in the tissues of *Drosophila melanogaster*. *Nucleic Acids Res.* 2013;41:D744–D750. [PubMed: 23203866]
23. Gibson J, Isaac R, Dinan L, Rees H. Metabolism of (3H)-ecdysone in *Schistocerca gregaria*: formation of ecdysteroid acids together with free and phosphorylated ecdysteroid acetates. *Arch Insect Biochem Phys.* 1984;1:385–407.
24. Ito Y, Yasuda A, Sonobe H. Synthesis and phosphorylation of ecdysteroids during ovarian development in the silkworm, *Bombyx mori*. *Zool Sci* 2008;25:721–727. [PubMed: 18828659]
25. Sonobe H, Ohira T, Ieki K, et al. Purification, kinetic characterization, and molecular cloning of a novel enzyme, ecdysteroid 22-kinase. *J Biol Chem.* 2006;281:29513–29524. [PubMed: 16899460]
26. Simon AF, Shih C, Mack A, Benzer S. Steroid control of longevity in *Drosophila melanogaster*. *Science.* 2003;299:1407–1410. [PubMed: 12610309]
27. Tricoire H, Battisti V, Trannoy S, Lasbleiz C, Pret AM, Monnier V. The steroid hormone receptor EcR finely modulates *Drosophila* lifespan during adulthood in a sex-specific manner. *Mech Ageing Dev.* 2009;130:547–552. [PubMed: 19486910]
28. Fluegel ML, Parker TJ, Pallanck LJ. Mutations of a *Drosophila* NPC1 gene confer sterol and ecdysone metabolic defects. *Genetics.* 2006;172:185–196. [PubMed: 16079224]
29. Huang X, Suyama K, Buchanan J, Zhu AJ, Scott MP. A *Drosophila* model of the Niemann-pick type C lysosome storage disease: *dnpc1a* is required for molting and sterol homeostasis. *Development.* 2005;132:5115–5124. [PubMed: 16221727]
30. Petryk A, Warren JT, Marques G, et al. Shade is the *Drosophila* P450 enzyme that mediates the hydroxylation of ecdysone to the steroid insect molting hormone 20-hydroxyecdysone. *Proc Natl Acad Sci USA.* 2003;100:13773–13778. [PubMed: 14610274]
31. Baer MM, Palm W, Eaton S, Leptin M, Affolter M. Microsomal triacylglycerol transfer protein (MTP) is required to expand tracheal lumen in *Drosophila* in a cell-autonomous manner. *J Cell Sci.* 2012;125:6038–6048. [PubMed: 23132924]
32. Jaspers MH, Pflanz R, Riedel D, Kawelke S, Feussner I, Schuh R. The fatty acyl-CoA reductase waterproof mediates airway clearance in *Drosophila*. *Dev Biol.* 2014;385:23–31. [PubMed: 24183938]

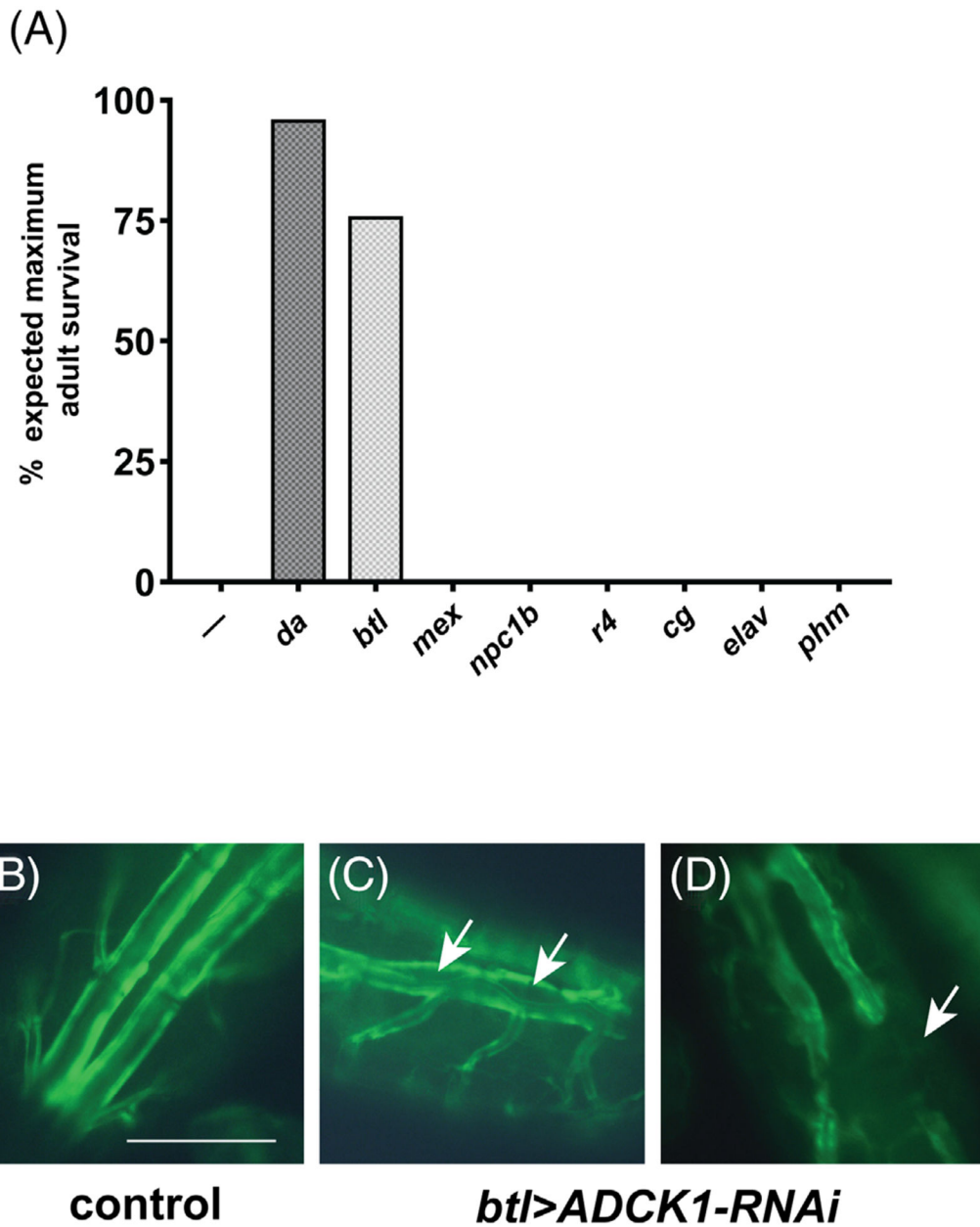
33. Ile KE, Tripathy R, Goldfinger V, Renault AD. Wunen, a *Drosophila* lipid phosphate phosphatase, is required for septate junction-mediated barrier function. *Development*. 2012;139:2535–2546. [PubMed: 22675212]
34. Tang X, Benesch MG, Brindley DN. Lipid phosphate phosphatases and their roles in mammalian physiology and pathology. *J Lipid Res*. 2015;56:2048–2060. [PubMed: 25814022]
35. Yoon W, Hwang SH, Lee SH, Chung J. *Drosophila* ADCK1 is critical for maintaining mitochondrial structures and functions in the muscle. *PLoS Genet*. 2019;15:e1008184. [PubMed: 31125351]
36. Gratz SJ, Ukken FP, Rubinstein CD, et al. Highly specific and efficient CRISPR/Cas9-catalyzed homology-directed repair in *Drosophila*. *Genetics*. 2014;196:961–971. [PubMed: 24478335]
37. Venken KJ, Bellen HJ. Genome-wide manipulations of *Drosophila melanogaster* with transposons, Flp recombinase, and PhiC31 integrase. *Methods Mol Biol*. 2012;859:203–228. [PubMed: 22367874]
38. Kumar S, Stecher G, Tamura K. MEGA7: molecular evolutionary genetics analysis version 7.0 for bigger datasets. *Mol Biol Evol*. 2016;33:1870–1874. [PubMed: 27004904]
39. Tennessen JM, Barry WE, Cox J, Thummel CS. Methods for studying metabolism in *Drosophila*. *Methods*. 2014;68:105–115. [PubMed: 24631891]

**FIGURE 1.**

Maximum likelihood phylogeny of ADCK family members. Reciprocal BLAST searches using the amino acid sequences for the five mammalian ADCK proteins were used to obtain homologous protein sequences from yeast, *Drosophila* and *Caenorhabditis elegans*. These sequences were aligned using MUSCLE software and the aligned peptide sequences were uploaded to MEGA7 to generate a maximum likelihood phylogram. Bootstrap values are shown at the branchpoints. The lengths of the bars represent the protein sequence divergence

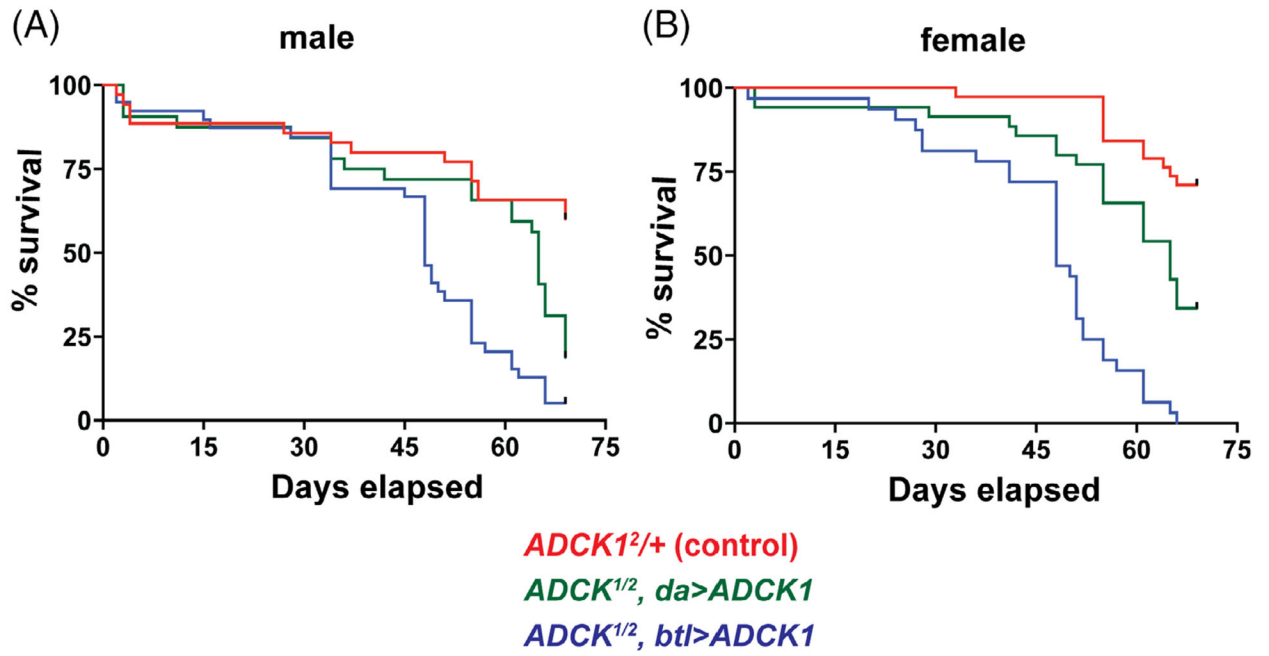
**FIGURE 2.**

*Drosophila ADCK1* mutants are larval lethal. A, The structure of the *ADCK1* locus is depicted along with the locations of the two deletion alleles. The deleted regions are replaced with an eye-specific *DsRed* reporter in both mutants. B,C, Transheterozygotes of *ADCK1*<sup>1/2</sup> mutants display second instar larval lethality with double mouth hooks, indicative of a molting defect. The first and second instar mouth hooks are labeled. Scale bar: 20  $\mu$ m. D,E, *ADCK1*<sup>1/2</sup> mutants display defects in tracheal morphology and tracheal breaks. Controls and mutants are depicted with representative images of the dorsal tracheal trunks. Panel E has an enlarged inset on the right. Scale bars: 0.25 mm (control), 0.2 mm (mutant)



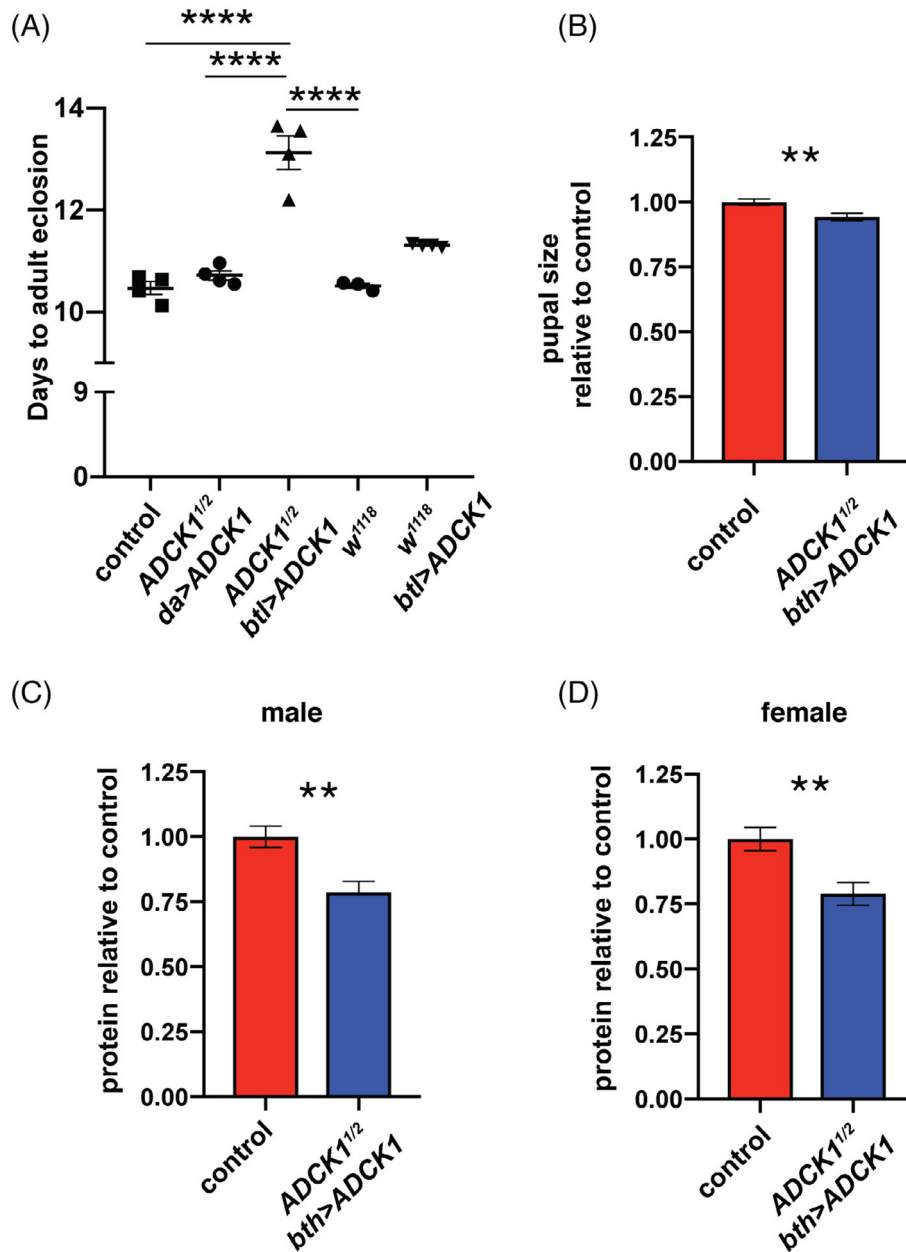
**FIGURE 3.**

*ADCK1* acts in the trachea to support larval viability. A, Tissue-specific GAL4 drivers listed on the x-axis were combined with the *UAS-ADCK1* transgene in an *ADCK1<sup>1/2</sup>* mutant background and scored for adult viability relative to *ADCK1* mutants alone (—). The efficiency of rescue is shown as a percentage of adult offspring relative to the expected value for full rescue. n = 200. Ubiquitous (*da-GAL4*), fat body (*cg-GAL4*, *r4-GAL4*), intestine (*mex-GAL4*, *npc1b-GAL4*), neuronal (*elav-GAL4*), tracheal (*btl-GAL4*), and prothoracic gland (*phm-GAL4*) drivers were used. B-D, Dorsal tracheal trunks were imaged from offspring obtained by crossing *btl-GAL4*, *UAS-GFP* to either *UAS-mCherry RNAi* (control, B) or *UAS-ADCK1-RNAi* (C,D). The arrows mark regions that display either abnormal tracheal morphology (C) or tracheal breaks (D). Scale bar = 0.25 mm

**FIGURE 4.**

Tracheal-rescued *ADCK1* mutant adults have a reduced lifespan. A,B, *ADCK1* mutants were rescued to adulthood using either the ubiquitous *da-GAL4* driver (green) or the tracheal-specific *btl-GAL4* driver (blue) and the lifespan of males (A) or mated females (B) was determined, along with genetically-matched controls (red). *P* values for the lifespan curves are: tracheal-rescued males compared to controls *P* .0001, tracheal-rescued females compared to controls *P* .0001, tracheal-rescued males compared to *da*-rescued males *P* .01, tracheal-rescued females compared to *da*-rescued females, *P* .0001, *da*-rescued males compared to controls *P* .01, *da*-rescued females compared to controls *P* .01. n = 35 flies for each genetic condition



**FIGURE 5.**

Tracheal-rescued *ADCK1* mutants are developmentally delayed and have reduced body size. A, Developmental delay was calculated for *w<sup>1118</sup>* animals, *w<sup>1118</sup>; ADCK1<sup>1/+</sup>* hemizygotes (control), ubiquitously-rescued mutants (*ADCK1<sup>1/2</sup> da > UAS-ADCK1*), tracheal-rescued mutants (*ADCK1<sup>1/2</sup> btl > UAS-ADCK1*), and control animals with tracheal-specific *ADCK1* overexpression (*w<sup>1118</sup>, btl > UAS-ADCK1*). The time required for 50% of the population to eclose is shown on the y-axis. Each data point represents results from one collection of animals (each collection n = 150) and the bars depict the mean  $\pm$  SEM. *P* values were calculated using one-way ANOVA with Tukey's multiple comparison test. B, Tracheal-rescued mutant pupae are smaller than controls. Pupal areas were measured and are presented as normalized to the size of *w<sup>1118</sup>* control pupae. C,D, Protein levels were

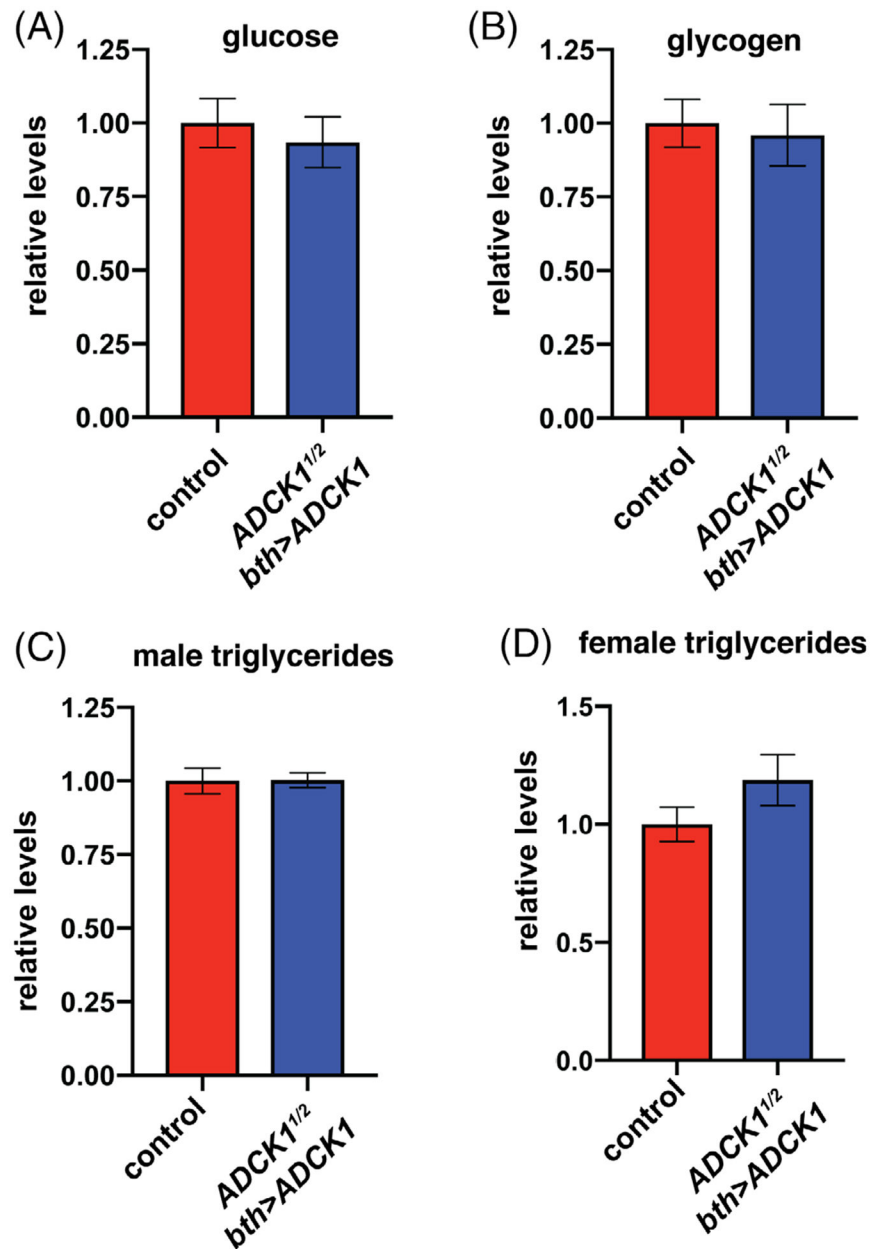
calculated using a Bradford assay in tracheal-rescued males (C) and females (D). Bars represent mean  $\pm$  SEM, n = 8 collections of five animals for each genotype. \*  $P < .05$ , \*\* $P < .01$ , \*\*\* $P < .0001$

Author Manuscript

Author Manuscript

Author Manuscript

Author Manuscript

**FIGURE 6.**

Tracheal-rescued *ADCK1* mutants have normal levels of basic metabolites. A-D, Glucose (A), glycogen (B), and triglycerides from males (C) or females (D) were measured in mature tracheal-rescued *ADCK1* mutant adults.  $n = 8$  for each sample. Metabolite levels are normalized to soluble protein levels and presented relative to the controls. Bars represent mean  $\pm$  SEM,  $n = 8$  (A),  $n = 20$  (B), and  $n = 15$  (C,D) collections of five animals for each genotype